Channel-Independent Synchronization of Orthogonal Frequency Division Multiple Access Systems

Sergio Barbarossa, *Member, IEEE*, Massimiliano Pompili, and Georgios B. Giannakis, *Fellow, IEEE*

***Abstract*—We develop synchronization algorithms for both the downlink and the uplink of quasi-synchronous and asynchronous orthogonal frequency division multiple access systems. Unlike existing alternatives, the proposed time- and carrier-offset estimators do not require the transmission of known sequences and exhibit performance independent of the underlying channel zero locations. The only necessary assumption is that there are virtual subcarriers which are not occupied by any user. We derive a closed-form variance expression for the carrier-offset estimator at high signal-to-noise ratio (SNR), as a function of the number of active users and the SNR. We compare our method with alternative ones and validate our theoretical derivations with simulation results.**

***Index Terms*—Multicarrier systems, multiple access, synchronization.**

I. Introduction

MULTIPLE access systems based on orthogonal frequency division multiplexing (OFDM) or, more generally, multicarrier (MC) modulation, are capable of insuring perfect elimination of multiuser interference (MUI) and intersymbol interference (ISI) in transmissions over time dispersive channels, using a very simple receiver. As opposed to CDMA systems, where MUI can be cancelled completely only resorting to computationally demanding multiuser detection (MUD) schemes [24], MC systems are able, in principle, to suppress MUI and ISI completely using a simple fast Fourier transform-based receiver [25]. This property is achieved by selecting a duration of the OFDM/MC block smaller than the channel coherence time, so that the channel can be considered stationary within one blocklength, and by inserting between any two successive transmitted blocks a cyclic prefix of duration at least equal to the channel order. However, different from CDMA, OFDM systems are much more sensitive to synchronization errors and to the nonlinearities of the transmitter high power amplifiers. This explains why, although OFDM has been successfully used in broadcasting systems, its generalization to multiple access systems, namely OFDMA, has not seen an equally widespread application yet, although it has been proposed for cable TV [18], broadband radio access networks [3] and for multiuser communications via satellite links [27].

Not surprisingly, synchronization of OFDM systems has received a lot of attention in the past [7], [12], [15] and several synchronization methods are available [1], [2], [8]–[12], [14], [16], [17], [19], [26]. All these works deal with single-user systems or with the broadcast channel and assume the transmission of a known sequence, or at least of two equal successive OFDM symbols. But, clearly, this entails a loss in information rate. To avoid this loss, in [21] it was proposed a method which exploited only the specific redundancy offered by the presence of cyclic prefix, but without sending pilot tones. The method of [21] was later extended to multiuser systems in [22]. The basic idea underlying [21], [22] is that in principle, in case of perfect synchronization and with ideal nondispersive channels, the first and last L samples of each block are equal to each other. More specifically, the authors of [21], [22] prove that their method approximates the optimum maximum-likelihood (ML) estimator, when the channel is ideal. However, when the channel is time-dispersive the performance of [21], [22] degrades considerably and, as shown in [21], the variance of the carrier offset estimate exhibits a floor at high signal-to-noise ratio (SNR).

In this paper, we propose a method which does not require the transmission of known training sequences, as in [21], whose major attribute, different from [21], is to have *channel-independent* performance. Our method capitalizes on the basic premise that the system is not fully loaded, i.e., not all available subcarriers are used for transmitting symbols. The proposed method exploits these null, or virtual, subcarriers to enforce time and frequency synchronization. Virtual subcarriers were also used by the *single-user* OFDM subspace-based methods in [10], [20]. However, the methods of [10], [20] suffer from an ambiguity problem arising if the channel transfer function has zeros at the edges of the frequency interval corresponding to the null subcarriers. Conversely, the method herein, unlike [10], [20], guarantees unambiguous carrier offset estimates with performance independent of the channel zeros location. Moreover, it is specifically devised for *multiuser* systems and it is simpler to implement than [10], [20] because it does not require any eigen-decomposition of the received signals. Even though the presence of virtual subcarriers can be seen as the transmission

Manuscript received December 16, 2000; revised May 21, 2001 and October 29, 2001. This work was supported in part by the Italian Ministry for the University and Scientific and Technological Research under the national project "OFDM Systems with Applications to WLAN Networks," in part by IST-1999-10322 SATURN project funded by the European Community (EC) and in part by the National Science Foundation (NSF) under Wireless Initiative Grant 9979443. Some of the results in this paper have been previously reported in M. Pompili, S. Barbarossa, G. B. Giannakis, "Channel-independent nondata aided synchronization of generalized multiuser OFDM," in *Proc. ICASSP 2001*, Salt Lake City, UT, May 2001, pp. 2341–2344, and in S. Barbarossa, M. Pompili, G. B. Giannakis, "Time and frequency synchronization of orthogonal frequency division multiple access system," in *Proc. ICC 2001*, Helsinki, June 2001, pp. 1674–1678.

S. Barbarossa is with the INFOCOM Department, University of Rome "La Sapienza," 00184 Rome, Italy (e-mail: sergio@infocom.uniroma1.it).

M. Pompili is with the Marconi Mobile, 00040 Pomezia, Rome, Italy (e-mail: massipom@libero.it).

G. B. Giannakis is with the Department of Electrical and Computer Engineering, University of Minnesota, Minneapolis, MN 55455 USA (e-mail: georgios@ece.umn.edu).

Publisher Item Identifier S 0733-8716(02)00996-4.

of known (null) symbols, there is a basic practical difference because the transmission of null symbols does not imply any waste of power. Furthermore, null subcarriers are intrinsically present in any nonfully loaded MC system (a situation which occurs most of the time).

The paper is organized as follows. In Section II, we start with the downlink channel and derive the received signal model for asynchronous and quasi-synchronous systems. In Section III, we propose our method for estimating the frequency offset in the downlink of quasi-synchronous systems and analyze its performance. In Section IV, we consider the time and frequency synchronization of the downlink of asynchronous systems. In Section V, we analyze the multiple access channel and, finally, in Section VI, we report simulation results to validate our theoretical findings and analyze the performance of our methods.

II. Broadcast Channel

We start with the broadcast, or downlink, channel and then we will consider the more challenging uplink channel in Section V.

A. Transmitted/Received Signal

We consider a block transmission from the base station (BS) to each mobile unit (MU) in a wireless MC multiuser system capable of accommodating a maximum of M users. Each transmitted block is composed of $N+L$ samples, where the first L samples are equal to the last L ones and, thus, constitute the cyclic prefix. The maximum number of orthogonal subcarriers is N. The number of subcarriers assigned to the mth user is J_m, with J_m possibly varying from user to user to allow for variable transmission rates and/or different bit-error rates (BERs). Denoting by M_a the number of simultaneously active users, the number of subcarriers really occupied for symbol transmission is $N_a = \sum_{m=1}^{M_a} J_m$. Hence, there are $N_v := N - N_a$ subcarriers which do not carry any symbol. We call these subcarriers *virtual*, or *null*, subcarriers. We enforce N_v to be strictly positive by preventing the users to occupy all possible subcarriers.

We denote with $u_m(p;l)$ the lth [possibly (pre)coded] symbol transmitted by the mth user within the pth block.[1] The number J_m of (coded) symbols $u_m(p;l)$ does not necessarily coincide with the number of information symbols per block (per user). For example, to increase resilience against frequency selective fading, it is better to take J_m greater than the number of information symbols. This can be obtained using a linear redundant precoder, as in [18], [5], and [25], or incorporating forward error correction coding before OFDM. Nevertheless, it is important to point out that the synchronization method proposed in this paper is neither restricted to any specific multiplexing or coding strategy, nor it assumes knowledge of the transmitted constellation or possible symbol correlation. To maintain the simplicity of notation, we will assign the same number of subcarriers $J \geq 1$ subcarriers to each user, but this is not a real limitation because, from the point of view of our synchronization method, the only necessary condition is that there is a nonempty set of virtual subcarriers.

[1]Throughout this paper, the first argument (e.g., p) will be the block index, while the second one (e.g., l) will denote the indexes within the block. Subscripts will index users.

We adopt a flexible assignment strategy for distributing subcarriers among users. Our strategy depends on the operational mode (down or uplink) and is aimed at striking the best compromise between frequency diversity gain and simplicity of the synchronization algorithm. In particular, in the broadcast channel, each symbol $u_m(p;l)$ is associated to a frequency index $m + lM + i_p$, where i_p is a frequency hopping index. Therefore, in the pth block, the set of frequency indexes assigned to user 0 is $[i_p, M+i_p, 2M+i_p, \ldots]$, the set assigned to user 1 is $[i_p+1, M+1+i_p, 2M+1+i_p, \ldots]$, and so on. This strategy insures maximum separation among the frequencies assigned to each user, but, at the same time, minimum separation among the sets of frequencies assigned to different users, which turn out to be interlaced. This choice yields maximum frequency diversity gain to each user. The hopping sequence $\{i_p\}_{p=0}^{N-1}$ is only required to explore the whole range $\{0, 1, \ldots, N-1\}$, but the sequence followed to explore this range is totally arbitrary. We will show in Section III-C that frequency hopping is instrumental to yield channel-independent performance of our estimator.

We model the channel as a linear time-invariant filter with impulse response strictly limited in time. To avoid interblock interference, we introduce at the beginning of each transmitted block, as in any OFDM system, a cyclic prefix whose length L is at least equal to the channel order. With these notations and assumptions, the pth block of length $N+L$ broadcasted from the BS has entries

$$x(p;n) = \sum_{m=0}^{M_a-1} \sum_{l=0}^{J-1} u_m(p;l) e^{j\frac{2\pi}{N}(m+lM+i_p)n}, \quad n \in [-L, N-1]. \quad (1)$$

Given the periodicity of order N of the complex exponentials in (1), the first L samples of $x(p;n)$ are equal to the last L ones.

B. Asynchronous Systems

We write now the expression of the sequence received by the kth user in an asynchronous system, in the presence of time and frequency offsets. Denoting with $g_T(t)$ and $g_R(t)$ the transmit and receive square-root Nyquist filters, respectively, and with $h_k(t)$ the continuous-time baseband channel between the BS and the kth user, the combined transmit-channel-receive filter impulse response is $c_k(t) := g_T(t) \star h_k(t) \star g_R(t) := c_k(t) \star g(t)$, where $g(t)$ is the combined impulse response $g(t) := g_T(t) \star g_R(t)$ and $\star$ denotes convolution. Hence, the baseband continuous-time waveform received by the kth user of interest is

$$y_k(t) = \sum_{p=-\infty}^{\infty} \sum_{n=-L}^{N-1} x(p;n) c_k(t - p(N+L)T - nT) \times e^{j2\pi f_k t} + v(t) \quad (2)$$

where $v(t)$ denotes additive noise, $1/T$ is the transmission rate and f_k is the carrier offset that arises from the mismatch between the BS and the kth user's oscillators. The first sum in (2) runs across successive blocks of length $N+L$, while the second sum operates within each block. The qth block collected by the kth user is composed of samples of $y_k(t)$ taken at instants $t = q(N+L)T + iT - \tau_k$, where τ_k is the time offset between the

BS and the kth user. Substituting (1) in (2), and sampling at rate $1/T$, the entries of the qth block of the kth user are then

$$y_k(q;i) = e^{j2\pi\bar{\nu}_k(q(N+L)+i)-\bar{\tau}_k)} \times \sum_{p=-\infty}^{\infty}\sum_{n=-L}^{N-1}\sum_{m=0}^{M_a-1}\sum_{l=0}^{J-1} u_m(p;l)e^{j\frac{2\pi}{N}(m+lM+i_p)n} \times c_k((q-p)(N+L)T+(i-n)T-\tau_k)+v(q;i) \quad (3)$$

where we have introduced the dimensionless offset variables $\bar{\nu}_k := f_kT$ and $\bar{\tau}_k := \tau_k/T$.

C. Quasi-Synchronous Systems

In quasi-synchronous systems, the MUs attempt to synchronize with a pilot signal sent by the BS, before initiating the communication link. As a consequence, the relative time-offsets among users are limited to a few chips (fraction of a symbol), and can, thus, be incorporated as part of the unknown channel impulse response. In such cases, the time offset is compensated as part of the equalization performed at the receiver. This approach entails a small efficiency loss, because it requires guard intervals longer than the channel delay spread (to account for the relative delays among users). However, it simplifies the synchronization task considerably, because it allows one to concentrate only on the carrier offsets. Incorporating the delays as part of the impulse responses $c_k(t)$ amounts to setting $\tau_k = 0$ in (3). In particular, we assume that the overall channels, including the delays, have at most duration LT, i.e., $c_k(t) \equiv 0$, for $t < 0$ or $t > LT, \forall k$. In this case, the only nonzero contribution of the sums over p in (3) and (21) comes from the qth term. Thus, setting $r = i - n$ in (3) and removing the cyclic prefix to avoid interblock interference, the resulting qth block of length N received at the kth MU of interest is given by

$$\begin{aligned} y_k(q;i) &= e^{j2\pi\bar{\nu}_k(q(N+L)+i)}\sum_{m=0}^{M_a-1}\sum_{l=0}^{J-1}u_m(q;l) \times \sum_{r=0}^{L}c_k(r)e^{j\frac{2\pi}{N}(m+lM+i_q)(i-r)}+v(q;i) \\ &= e^{j2\pi\bar{\nu}_k(i+q(N+L))} \times \sum_{m=0}^{M_a-1}\sum_{l=0}^{J-1}\tilde{u}_{m,k}(q;l)e^{j\frac{2\pi}{N}(m+lM+i_q)i}+v(q;i), \\ & \qquad i \in [0,\ldots,N-1] \end{aligned} \quad (4)$$

where $\tilde{u}_{m,k}(q;l) := u_m(q;l)C_k(m+lM+i_q)$, having introduced the kth channel's transfer function $C_k(l) := \sum_{r=0}^{L} c_k(r)e^{-j((2\pi)/N)lr}, l \in [0, N-1]$.

III. Frequency Synchronization

We describe now our frequency synchronization algorithm for quasi-synchronous systems. We explain our synchronization algorithm with reference to Fig. 1, where the upper branch shows the basic building blocks of an OFDM receiver; namely, sampling, carrier offset compensation, serial to parallel (S/P) conversion to form blocks of N data, and FFT, equalization and detection. The novelty lies in the algorithm for estimating and compensating both time and frequency offsets, described through the blocks in the lower branch of Fig. 1. In this section, we focus on frequency synchronization, even though the scheme of Fig. 1 incorporates the time offset compensation, whose description we postpone to Section IV.

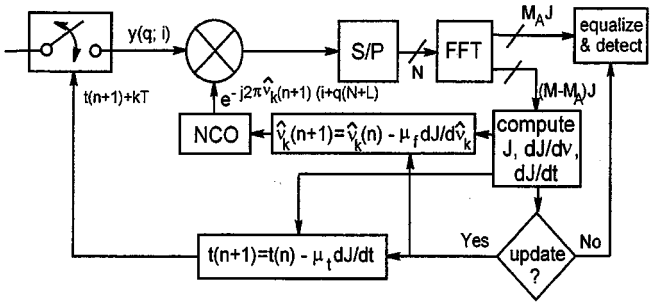

Fig. 1. Block diagram of the proposed OFDM receiver.

Our *basic idea* for synchronization is fairly simple: We measure the average energy falling across the N_v virtual subcarriers and update the oscillator frequency until we reach a minimum of the measured energy. Ideally, in case of perfect synchronization and no noise, we should observe a null energy. If we detect some energy, we update the receiver oscillator in order to minimize such energy. Correspondingly, the synchronization algorithm is rather simple. We run an iterative search which yields the frequency offset that minimizes the energy falling in the band corresponding to the virtual subcarriers. Denoting with $\tilde{\nu}_k(n)$ our estimate of the frequency offset, obtained at the nth iteration, we start with an initial guess $\tilde{\nu}_k(0)$ and, in each step we compensate each received block by multiplying it by the sequence $e^{-j2\pi\tilde{\nu}_k(n)(i+q(N+L))}$ generated by the numerically controlled oscillator (NCO), as shown in Fig. 1, thus yielding[2]

$$\begin{aligned} \tilde{y}(q;i) &:= y(q;i)e^{-j2\pi\tilde{\nu}_k(i+q(N+L))} \\ &= e^{j2\pi\nu_k(i+q(N+L))}\sum_{m=0}^{M_a-1}\sum_{l=0}^{J-1}\tilde{u}_{m,k}(q;l) \times e^{j\frac{2\pi}{N}(m+lM+i_q)i}+\tilde{v}(q;i) \end{aligned} \quad (5)$$

where $\nu_k := \bar{\nu}_k - \tilde{\nu}_k$ and $\tilde{v}(q;i) := v(q;i)e^{-j2\pi\tilde{\nu}_k(i+q(N+L))}$. Then, following the scheme in Fig. 1, we evaluate the FFT of the qth block $\tilde{y}(q;i)$:

$$Y_{m'}(q;l') := \frac{1}{N}\sum_{i=0}^{N-1}\tilde{y}(q;i)e^{-j\frac{2\pi}{N}(m'+l'M+i_q)i}, \quad m' \in [0, M-1], \quad l' \in [0, J-1]. \quad (6)$$

Substituting (4) into (6), we obtain

$$\begin{aligned} Y_{m'}(q;l') &= \frac{1}{N}e^{j2\pi\nu_k q(N+L)}\sum_{m=0}^{M_a-1}\sum_{l=0}^{J-1}\tilde{u}_{m,k}(q;l) \times \frac{\sin[\pi(m-m'+(l-l')M+\nu_k N)]}{\sin\{[\pi(m-m'+(l-l')M+\nu_k N)]/N\}} \\ &\quad \cdot e^{j\pi(m-m'+(l-l')M+\nu_k N)(N-1)/N}+V_{m'}(q;l') \end{aligned} \quad (7)$$

where $V_{m'}(q;l') := (1/N)\sum_{i=0}^{N-1} v(q;i)\exp(-j2\pi(m'+l'M+i_q)i/N)$ is the FFT output noise, which remains

[2]We drop the dependence of $\bar{\nu}_k(n)$ and $\tilde{\nu}_k(n)$ on the iteration index n, for simplicity of notation.

zero-mean white complex Gaussian (even after FFT processing) with variance $\sigma_V^2 = \sigma_v^2/N$.

In case of perfect synchronization, i.e., $\nu_k = 0$, and no noise, the ratio in (7) is different from zero (and equal to N) only for $m' = m$ and $l' = l$, so that

$$Y_{m'}(q;l') = \begin{cases} \tilde{u}_{m',k}(q;l'), & \text{for } m' \in [0, M_a - 1] \quad \text{and} \quad l' \in [0, J-1] \\ 0, & \text{otherwise.} \end{cases} \tag{8}$$

Equation (8) confirms, as expected, that perfect synchronization leads to zero MUI/ISI among OFDM symbols and null energy in the band not occupied by information symbols. Conversely, in case of nonperfect synchronization, the summations in (7) evidence the presence of MUI/ISI and of a nonnull energy also in correspondence with the null subcarriers.

A. Cost Function

Exploiting this last observation, our carrier synchronization method yields the offset which minimizes the average energy of $Y_{m'}(q;l';\nu_k)$ falling on the null subcarriers. Specifically, we introduce the cost function $\mathcal{J}_{N_b}(\nu_k)$ measuring the energy falling in the band pertaining to the virtual subcarriers averaged over N_b blocks

$$\mathcal{J}_{N_b}(\nu_k) := \frac{1}{N_b} \sum_{q=0}^{N_b-1} \sum_{m'=M_a}^{M-1} \sum_{l'=0}^{J-1} |Y_{m'}(q;l')|^2 \tag{9}$$

and we estimate $\hat{\nu}_k$ as the value that minimizes $\mathcal{J}_{N_b}(\nu_k)$, i.e.,

$$\hat{\nu}_k = \arg\min_{\nu_k} J_{N_b}(\nu_k). \tag{10}$$

In case of perfect synchronization and no noise, recalling (8), the cost function in (9) is identically null. Conversely, in the presence of carrier offset and noise, $\mathcal{J}_{N_b}(\nu_k)$ is composed of a noise contribution plus some energy falling in the null guard interval because of the frequency offset. We will show next that $\mathcal{J}_{N_b}(\nu_k)$ reaches asymptotically (i.e., for $N_b \to \infty$) its absolute minimum only at $\nu_k = 0$.

Let us define $\mathcal{J}(\nu_k) := \lim_{N_b \to \infty} \mathcal{J}_{N_b}(\nu_k)$. Assuming that the transmitted sequence is ergodic, the sample average in (9) tends to its ensemble counterpart, as $N_b \to \infty$. For simplicity, we also assume the symbols $u_m(p;l)$ to be uncorrelated, even though our derivations can be readily extended to the correlated case. Define $N_p := N_b/N$ and set $q = pN + r$ in (9), with $p = 0, \ldots, \infty$ and $r = 0, \ldots, N-1$. For a fixed N, as $N_b \to \infty$ (or equivalently $N_p \to \infty$), exploiting the ergodicity of $u_m(q;l)$ we obtain (11), shown at the bottom of the page, where the expected value operator $E\{\cdot\}$ is taken over both the symbol sequence and the additive noise. The whiteness of $u_m(p;l)$ implies that $E\{u_m^*(p;l)u_{m'}(p;l')\} = \sigma_u^2 \delta[l-l']\delta[m-m']$, which after substituting (7) in (11) leads to (12), shown at the bottom of the page, where $\mathrm{sinc}_N(x) := \sin(\pi x)/\sin(\pi x/N)$. At this point, we exploit the subcarrier hopping sequence i_r that we designed to take all the values $\{0, 1, \ldots, N-1\}$, as r goes from 0 to $N-1$. Considering that the channel transfer function $C(m)$ is periodic, with period N, the sum $(1/N)\sum_{r=0}^{N-1} |C_k(m + lM + i_r)|^2 := C_k^2$ depends neither on m nor on l. Therefore, we can re-write (12) as shown in (13) at the bottom of the page. Four important remarks follow immediately from (13).

Remark 1: Since $\mathcal{J}(\nu_k)$ is given by the sum of nonnegative terms, its absolute minimum is reached when all the terms $\mathrm{sinc}_N^2(\cdot)$ are null. This situation occurs only when $\nu_k = 0$, which represents then the unique absolute minimum[3]

Remark 2: The cost function depends on the channel impulse response only through the multiplicative scalar C_k^2. This proves that our carrier synchronization method has performance *independent of the channel zero locations*. This property is achieved thanks to subcarrier hopping from block to block. Intuitively speaking, as we take the average over N_b consecutive blocks, thanks to FH, we are, equivalently, averaging over frequency. Furthermore, due to the specific FH we have incorporated, for each set of N blocks, we are averaging over the whole available spectrum. This is why the performance is independent of the channel selectivity and depends on the channel only through a multiplicative coefficient.

[3]If $\nu_k = k/N$, with k nonnull integer, some $\mathrm{sinc}_N(\cdot)$ functions are also null, but not all of them. In this cases, we have then relative minima, but not the absolute minimum.

$$\mathcal{J}(\nu_k) = \lim_{N_p \to \infty} \frac{1}{NN_p} \sum_{p=0}^{N_p-1} \sum_{r=0}^{N-1} \sum_{m'=M_a}^{M-1} \sum_{l'=0}^{J-1} |Y_{m'}(pN+r;l')|^2 = \frac{1}{N} \sum_{r=0}^{N-1} \sum_{m'=M_a}^{M-1} \sum_{l'=0}^{J-1} E\{|Y_{m'}(r;l')|^2\} \tag{11}$$

$$\mathcal{J}(\nu_k) := \frac{\sigma_u^2}{N^3} \sum_{r=0}^{N-1} \sum_{m'=M_a}^{M-1} \sum_{l'=0}^{J-1} \sum_{m=0}^{M_a-1} \sum_{l=0}^{J-1} |C_k(m+lM+i_r)|^2 \mathrm{sinc}_N^2[m-m'+(l-l')M+\nu_k N] + \sigma_v^2 \frac{M-M_a}{M} \tag{12}$$

$$\mathcal{J}(\nu_k) := \frac{\sigma_u^2 C_k^2}{N^2} \sum_{m'=M_a}^{M-1} \sum_{l'=0}^{J-1} \sum_{m=0}^{M_a-1} \sum_{l=0}^{J-1} \mathrm{sinc}_N^2[m-m'+(l-l')M+\nu_k N] + \sigma_v^2 \frac{M-M_a}{M} \tag{13}$$

Remark 3: The carrier offset estimator in (10) is mean-square sense *consistent*, i.e., as the number of blocks $N_b \to \infty$, the noise is not going to affect the estimate. In fact, we observe from (13) that the only effect of the additive white noise (that is assumed uncorrelated from the useful signal), is to add a pedestal to the cost function and, thus, it does not alter, the position of the global minimum of $\mathcal{J}(\nu_k)$.

Remark 4: Analyzing the behavior of $\mathcal{J}(\nu_k)$ in the neighborhood of $\nu_k = 0$, we can verify that the width of the global minimum is approximately $1/NT$ Hz [4]. Hence, any iterative carrier offset estimation algorithm is guaranteed to converge to the global minimum, provided that the initial frequency offset is less than $1/2NT$, in modulus. If the initial offset has magnitude greater than $1/2NT$, one has to try multiple initializations with initial carriers differing by integer multiples of $1/NT$, and take the estimated carrier offset resulting from the initialization that yields the minimum cost function.

B. Estimation Algorithm

We use a conventional steepest-gradient-descent algorithm for estimating the carrier offset ν_k. Specifically, with reference to Fig. 1 the qth received block $y(q;i)$ is multiplied, at the nth step, by $\exp(-j2\pi\hat{\nu}_k(n)(i+q(N+L)))$, to form $\tilde{y}(q;i) := y(q;i)\exp(-j2\pi\hat{\nu}_k(n)(i+q(N+L)))$, where $\hat{\nu}_k(n)$ is the carrier offset estimate at step n. The algorithm starts with $\hat{\nu}_k(0) = 0$ as an initial estimate, and utilizes a sample-averaged gradient-based steepest-descent iteration in order to minimize the cost function in (9). At the nth step, the algorithm estimates the cost function $\mathcal{J}(\hat{\nu}_k(n))$ and its gradient $\partial\mathcal{J}(\hat{\nu}_k(n))/\partial\hat{\nu}_k(n)$, by averaging over a finite number of blocks $N_b = N_pN$. At each step we evaluate the cost function and its gradient. If the modulus of the gradient exceeds a threshold, we update our estimate as follows:

$$\hat{\nu}_k(n+1) = \hat{\nu}_k(n) - \mu\frac{\partial\mathcal{J}(\hat{\nu}_k(n))}{\partial\hat{\nu}_k(n)} \tag{14}$$

otherwise we exit from the loop. The step size μ is (as with any steepest-descent method) selected as a compromise between convergence speed and tracking capability. We show in the Appendix B that, in the asymptotic case where $N_b \to \infty$, the algorithm is guaranteed to converge provided that the step size is chosen to satisfy: $0 < \mu < 2/\lambda$, where λ is given by (37). In practice, when a finite number of blocks is used, it is safer to use a smaller value of λ with respect to (37). To reduce the complexity of the algorithm, the average gradient in (14) can also be replaced by its instantaneous (stochastic) approximation. In such a case, the maximum value of μ must be further reduced to avoid divergence of the algorithm.

[4]We measure the null width as twice the distance from the null to the first value where the function reaches half of its maximum value.

C. Performance Analysis of Carrier Frequency Estimation

In this section, we derive an approximate analytic expression for the variance of $\hat{\nu}_k$ in (10). We use a small perturbation analysis, approximately valid for high SNR and for any number of data used in the synchronization algorithm. Let us denote by $J_s(\nu)$ and $J_{s+w}(\nu)$ the cost functions in the absence and presence of noise, respectively (in order to avoid an unnecessary overcrowding of the formulas we will, henceforth, drop the indexes for the users and the number of blocks). The perturbation induced by the noise is, thus, $\delta J_{s+w}(\nu) := J_{s+w}(\nu) - J_s(\nu)$. In the presence of noise, the carrier offset estimate is the value ν which minimizes $J_{s+w}(\nu)$. Therefore, ν satisfies the following:

$$\frac{dJ_{s+w}(\nu)}{d\nu} = \frac{dJ_s(\nu)}{d\nu} + \frac{d\delta J_{s+w}(\nu)}{d\nu} = 0. \tag{15}$$

Taking the first-order Taylor expansion of (15) around the correct value $\nu = 0$, we have

$$\frac{dJ_s(0)}{d\nu} + \frac{d^2J_s0)}{d\nu^2}\nu + \frac{d\delta J_{s+w}0)}{d\nu} + \frac{d^2\delta J_{s+w}(0)}{d\nu^2}\nu = 0. \tag{16}$$

The first term in left-hand side of (16) is clearly zero and, if we retain only the first-order perturbation terms, we can neglect the last term of (16), so that the first-order approximation of the frequency estimation error is

$$\nu \simeq -\frac{\frac{d\delta J_{s+w}(0)}{d\nu}}{\frac{d^2J_s(0)}{d\nu^2}}. \tag{17}$$

At a first-order approximation, the expected value of ν is zero, which implies that the estimator is unbiased. The variance of (17) is derived in Appendix A and is equal to (18), shown at the bottom of the page, where $\mathrm{SNR} := \sigma_u^2C^2/\sigma_v^2$. Not surprisingly, since the method is based on the minimization of a cost function independent on the channel zero location, the variance is also independent of the channel selectivity. This is one of the most distinguishing features of our algorithm with respect to the available ones. We will verify the validity of (18) in Section VI using simulation results.

IV. Time and Frequency Synchronization of Asynchronous Systems

In this section, we extend our synchronization algorithm to asynchronous systems, where the time offset is not incorporated as part of the unknown channel impulse response and it has to be estimated separately. The basic idea is similar to the previous case, except that now we have two unknown parameters to estimate. More specifically, we estimate the time and frequency offsets as the values that minimize the cost function defined as

$$\sigma_\nu^2 = \frac{\sum_{n=0}^{M-1}\sum_{p=0}^{M-1}\sum_{q=0}^{M-1}(n-p)(q-p)\,\mathrm{sinc}_{M_a}\left(\frac{\pi M_a(n-q)}{M}\right)\mathrm{sinc}_{M_a}\left(\frac{\pi M_a(n-p)}{M}\right)\mathrm{sinc}_{M_a}\left(\frac{\pi M_a(p-q)}{M}\right)}{2\pi^2J^4\mathrm{SNR}\sum_{n=0}^{M-1}\sum_{p=0}^{M-1}(n-p)^2\mathrm{sinc}_{M_a}^2\left(\frac{\pi M_a(n-p)}{M}\right)} \tag{18}$$

in (9), with $Y_{m'}(q;l')$ given by (6), and $y(q;i)$ given now by (3), rather than (4). As depicted in Fig. 1, we need now two interlaced loops for estimating both time and frequency offsets. We start analyzing the asymptotic properties of the cost function and then we will provide a low-complexity (albeit suboptimal) synchronization method.

A. Cost Function

The behavior of the cost function is more complicated in the asynchronous case, because of the interference occurring between successive OFDM blocks whenever the sum of the channel order and the time offset exceeds the cyclic prefix length. The major consequence of this interblock interference is that the cost function now becomes channel dependent. To grasp some of the basic features of the joint synchronization algorithm, it is useful to show the behavior of the cost function in the ideal channel case, which can be derived in closed form. Specifically, in the ideal channel case, considering a guard interval of length L, after a few tedious, but otherwise straightforward, algebraic manipulations, we obtain

$$J(\nu,\theta)=\frac{\sigma_u^2}{N^2}\sum_{k=1}^{M-1}\sum_{l=-J+1}^{J-1}(J-|l|)\times\min(k,M-k,M_a,M-M_a)A(k,l,\nu,\theta) \quad (19)$$

where the equation shown at the bottom of the page holds.

We consider only values of time offsets $\theta\in[-N/2,N/2]$, because when θ falls outside that interval, there is an ambiguity about which symbol is being observed. This ambiguity can be resolved only by using extra information; e.g., by transmitting a known symbol at the beginning of the frame. To explain some of the basic properties of the asymptotic cost function, in Figs. 2 and 3, we report two examples of the cost function obtained using the following parameters: $M=8$, $L=4$,$J=8$, $N=MJ=64$, with $M_a=3$ in Fig. 2 and $M_a=7$ in Fig. 3. In Figs. 2 and 3, panels (a) show the mesh plot of $J(\nu,\theta)$, whereas panels (b) show two slices of $J(\nu,\theta)$, cut along the axes $\nu=0$ and $\theta=0$.

From Figs. 2 and 3, we can draw a few important remarks.

Remark 5: The 2-D shape of $J(\nu,\theta)$ in the neighborhood of the origin suggests that one should be able to decouple time from frequency offset estimation without performance loss, provided that the initial offset pair (ν,θ) falls within the rectangle $[-1/2N,1/2N;-N/2,N/2]$. Certainly, decoupling will influence the convergence rate, but it simplifies the synchronization considerably.

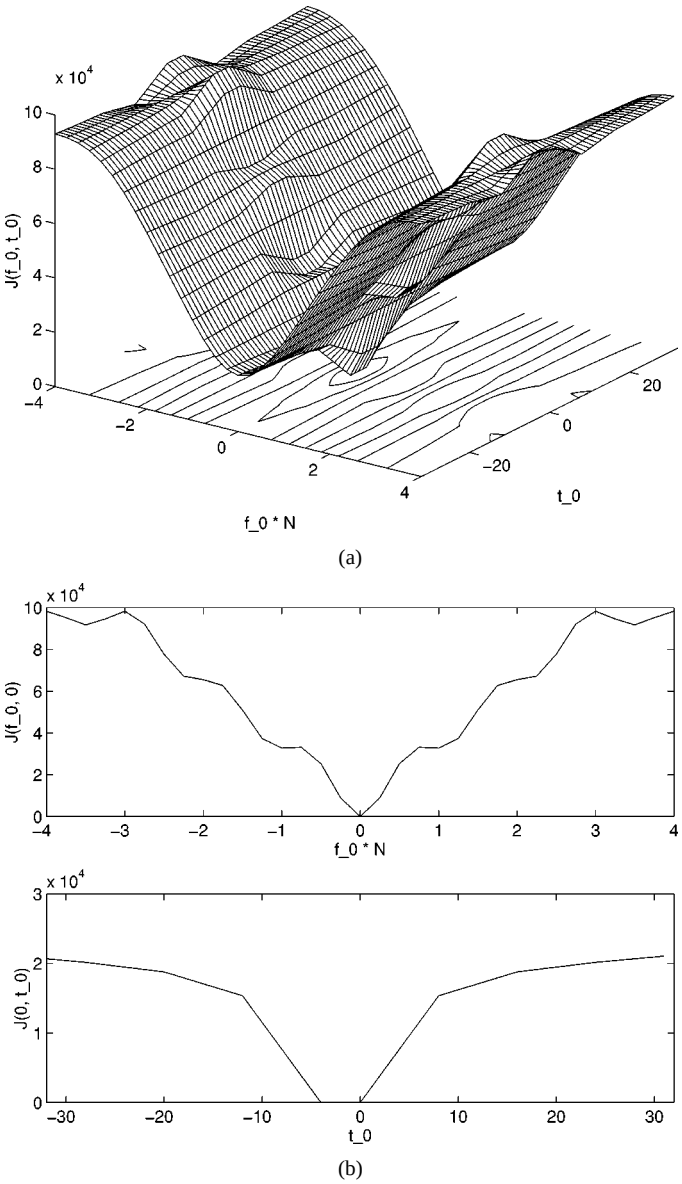

Fig. 2. Two-dimensional (2-D) cost function: $M=8$, $M_a=3$, $L=4$, and $J=8$.

Remark 6: The curve $J(\nu,0)$ is zero only when $\nu=0$ and the null width is approximately $1/N$, as in the quasi-synchronous case.

Remark 7: The curve $J(0,\theta)$ is null not only for $\theta=0$, but for all values $-L\le\theta\le 0$, i.e., for all time offsets falling within the guard interval, and it is monotonically increasing on both sides of that interval. This remark reflects the fact that if instead of being synchronous, we anticipate our initial time instant by a few chips, but we still remain inside one block (e.g.,

$$A(k,l,\nu,\theta):=\begin{cases}\mathrm{sinc}^2_{N-\theta}[(k+lM-\nu N)(N-\theta)/N]+\mathrm{sinc}^2_{\theta}[(k+lM-\nu N)\theta/N], & 0<\theta<N/2\\ \mathrm{sinc}^2_{N}(k+lM-\nu N), & -L\le\theta\le 0\\ \mathrm{sinc}_{\theta+L}[(k+lM-\nu N)(\theta+L)/N]+\mathrm{sinc}_{N+\theta+L}[\pi(k+lM-1-\nu N)(N+\theta+L)/N], & -\frac{N}{2}\le\theta<-L.\end{cases}$$

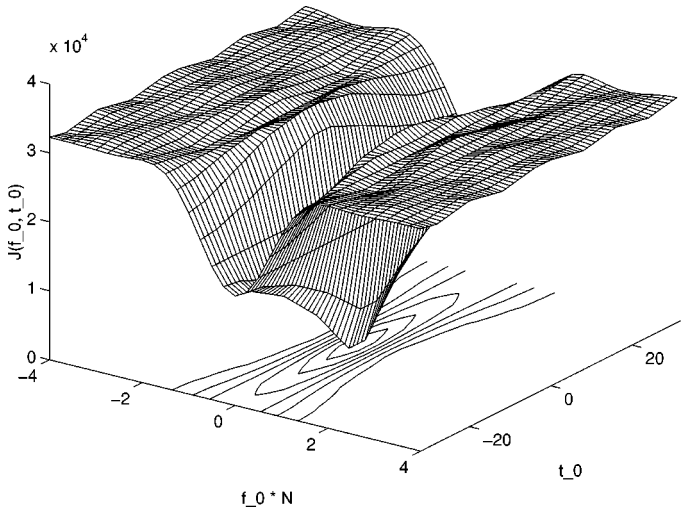

(a)

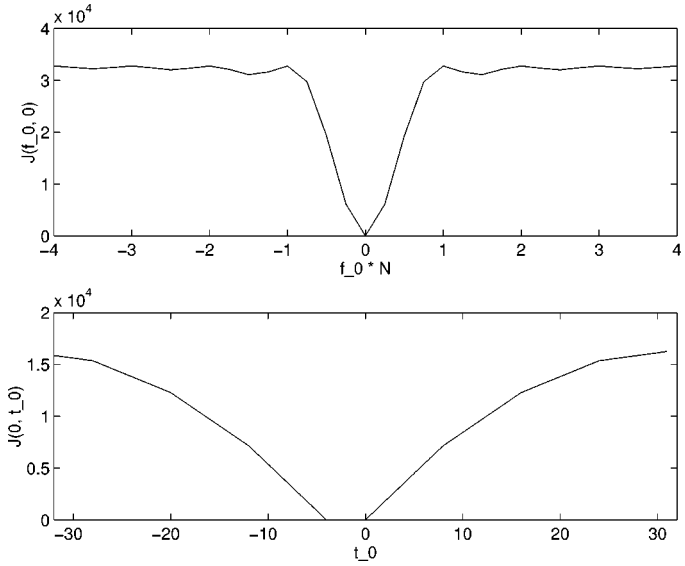

(b)

Fig. 3. Two-dimensional cost function: $M = 8$, $M_a = 7$, $L = 4$, and $J = 8$.

we do not take samples from different blocks in evaluating our cost function), in the absence of frequency offset, the null subcarriers are still orthogonal to the subcarriers occupied by the users. The existence of a nonunique null of $J(0, \theta)$ evidences a potential ambiguity problem in the estimation of the time offset. However, this is not a real problem which we have to worry about, because it is automatically compensated as part of the equalization process. In fact, if the residual time offset is equal to a fraction of L, the channel estimated at the output of the FFT will incorporate an extra linear phase exponential taking into account the uncompensated delay. Hence, when we divide the samples at the output of the final FFT in Fig. 1, by the estimated channel transfer function, this operation will remove not only the multipath but also the effect of the residual time offset (provided that $-L \leq \theta \leq 0$).

In the more general case, where the channel is not ideal, it is more difficult to derive a closed form expression for the cost function. To study the behavior of the cost function in such a case, we proceeded by simulation, modeling the channel as an finite impulse response filter (FIR) whose coefficients are Gaussian independent random variables (Rayleigh fading model), and computed the cost function using (9). In general, we verified that the only appreciable difference induced by the FIR channel is that the main null tends to be filled (mainly because of interblock interference), and the only point where $J(\nu, \theta)$ is always zero, regardless of the channel, is the origin.

B. Time Synchronization

The joint estimation of time and frequency offset can be obtained by computing the derivatives of $J(\nu, \theta)$ with respect to both ν and θ and then updating our estimates according to a 2-D steepest-descent algorithm. At each step of the algorithm, once we have our running estimates $\hat{\nu}(n)$ and $\hat{\theta}(n)$, we have to resample the continuous time received signal by shifting the initial sampling instant by $\hat{\theta}(n)$ and then compensating the frequency offset by multiplying each received block by $\exp(-j2\pi\hat{\nu}(n)(i + q(N + L)))$, as shown schematically in Fig. 1. In an all-digital implementation, this requires an oversampling of the received data. However, the joint estimation algorithm can be simplified considerably if we content ourselves with a granularity of our time offset estimate equal to the duration of a chip. In such a case, we can avoid oversampling and estimate the time offset as the value that minimizes the cost function. More specifically, we evaluate the cost function $J(\nu, \theta)$ for $\theta = k$, with $k = -N/2, \ldots N/2$, and estimate the time offset as $\hat{\theta} = \arg\min_k J(\nu, k)$. Once we have found $\hat{\theta}$, we apply the frequency synchronization algorithm described in Section III to the data synchronized in time. This overall procedure is suboptimum and it assumes that the time and frequency offsets can be estimated sequentially, as opposed to jointly. This assumption holds true only if at the beginning of our synchronization method, our initial errors are such that we are within the main null of the function $J(\nu, \theta)$, i.e., if the initial frequency error is smaller than $1/2N$, in modulus, and the initial time error is smaller than $N/2$, in modulus.

V. Multiple Access Channel

As far as the synchronization of the uplink channel is concerned, the situation changes considerably depending on the channel time variation. In fact, if the access channels are practically time-invariant, so that the frequency offset is only due to the oscillators drifts, the synchronization performed at each MU may be sufficient to avoid any further synchronization at the BS. However, if the users are moving and the main cause of lack of synchronization is Doppler shift, it is necessary to run the synchronization algorithm also at the BS. This case is much more complicated than the downlink case, because the signal received at the BS contains $2M_a$ unknowns: the time and frequency offsets of each active user. In an effort to simplify as much as possible the synchronization in this case, we change the rule for assigning the set of frequencies to each user. In particular, we assign the frequencies so that each user has now a set of contiguous frequencies and the distance between the spectra allocated to different users is maximized. Specifically, in the pth block, we assign to the mth user the set of frequency indexes: $(mJ_a + i_p, mJ_a + 1 + i_p, \ldots, mJ_a + J - 1 + i_p)$, where

$J_a := J + J_0$ and $J_0 := \lfloor (M - M_a)J/M_a \rfloor$ represents now the null gap between neighboring users' spectra. In formulas, the pth block transmitted from the mth MU assumes the form

$$x_m(p;n) = \sum_{l=0}^{J-1} u_m(p;l) e^{j\frac{2\pi}{N}(l+mJ_a+i_p)n}, \quad n = -L, \ldots, N-1. \quad (20)$$

This choice is not optimal with respect to frequency diversity, but it offers the maximum separation among the spectra allocated to different users. Compared with the downlink allocation in (1), the distance between each user's subcarriers is now minimum, but the guard interval separating the spectra of different users is maximized. This creates a "cushion" between neighboring users' spectra which facilitates the synchronization task, as described next. After pulse shaping with $g_T(t)$ and up-converting the $x_m(p;n)$ of (20), the transmission from the mth MU propagates through its own frequency-selective channel $h_m(t)$ and it is filtered at the BS with the receive-filter $g_R(t)$. Letting $c_m(t) := g_T(t) \star h_m(t) \star g_R(t)$ denote as before the combined impulse response from the mth MU to the BS, we again sample the received continuous-time waveform $y_m(t)$ at the symbol rate $1/T$, to obtain the sequence of blocks $y_m(q;i)$. Superimposing all such sequences received at the BS from the M_a users, we arrive at the following baseband discrete-time equivalent input-output relationship for a completely asynchronous uplink

$$y(q;i) = \sum_{p=-\infty}^{\infty} \sum_{n=-L}^{N-1} \sum_{m=0}^{M_a-1} \sum_{l=0}^{J-1} u_m(p;l) \times e^{j\frac{2\pi}{N}(l+mJ_a+i_p)n} c_m(((q-p)(N+L)+i-n-\tau_m)T) \times e^{j2\pi\bar{\nu}_m(q(N+L)+i)-\bar{\tau}_m)} + v(q;i). \quad (21)$$

For quasi-synchronous systems, after removing the cyclic prefix, we can express the qth block of N samples received at the BS from all M_a active users as

$$y(q;i) = \sum_{m=0}^{M_a-1} e^{j2\pi\bar{\nu}_m(q(N+L)+i)} \times \sum_{l=0}^{J-1} \tilde{u}_m(q;l) e^{j\frac{2\pi}{N}[(l+mJ_a+i_q)i]} + v(q;i), \quad i \in [0, \ldots, N-1] \quad (22)$$

where $\tilde{u}_m(q;l) := u_m(q;l) C_m(l+mJ_a+i_q)$. Given $y(q;i)$, our goal is now to estimate and compensate for the time- and carrier-offsets $\bar{\tau}_k$ and $\bar{\nu}_k$ of each user. Generalizing the approach followed in the downlink case, we can introduce a cost function that measures the average energy falling in the null frequency bands. However, as stated before, the minimization of the new cost function would be much more complicated because of the higher number of unknowns (M_a unknown frequencies for quasi-synchronous systems and $2M_a$ unknowns for asynchronous systems). In this paper, we consider only the synchronization of quasi-synchronous systems, so that the only unknowns are the M_a frequency offsets. We have simplified the estimate considerably by exploiting the specific structure of the signals transmitted from each user. Specifically, we first filter the received signal through a bank of bandpass filters, each one tuned to isolate a specific user. If the frequency offset of each MU is small enough with respect to the spectral gap between the spectra pertaining to different users, the filtering is sufficient to separate (approximately) the users. This allows us to apply a separate synchronization algorithm for each user. Clearly, since the filtering operation cannot be perfect, because of the different frequency offsets, we will have MUI and, thus, a performance loss with respect to the downlink case. We will quantify this loss by simulation in Section VI. To limit this loss, we have to increase the gap between different users, but this would reduce the number of users that have access to the system and it is the major price for synchronization in a time-varying scenario. However, it is worth saying that, as soon as the system improves its synchronization, we can decrease the guard intervals and, thus, allow access to additional users.

VI. Performance and Concluding Remarks

In the following, we show some numerical examples to verify the validity of our theoretical expressions and evaluate the overall performance of our OFDMA system.

Example 1 (Frequency Estimation in Downlink Channel): We have simulated a downlink channel transmission, with time and frequency offsets and parameters $M = 8$, $L = 2$, $J = 8$, and $N = MJ = 64$. We have estimated the time offset first, with a granularity T, using the method described in Section IV, and then we have run the steepest-descent method described in Section III to estimate the frequency offset. In Fig. 4, we report the variance of the frequency estimate obtained using (18) (solid line) and via Monte-Carlo simulations (circles), for the downlink channel, as a function of SNR [Fig. 4(a)] and M_a [Fig. 4(b)]. From Fig. 4(a), we observe that for SNR above 15 dB, i.e., for values of SNR necessary in any case to guarantee a reasonable BER, (18) is able to predict the simulation results very well, in spite of the unknown time offset. The explanation for this behavior is that at high SNR, there are practically no errors in estimating the integer time shifts. In Fig. 4(b), we show the estimation variance as a function of M_a, for a given SNR and we can observe that the variance reaches its minimum value for $M_a = M/2$.

Example 2 (Comparison With [21]): We compare now our frequency estimation method for the downlink channel with the method of [21]. Since our method assumes the presence of virtual subcarriers, whereas the method of [21] does not, to have a fair comparison we have to enforce the two systems to have the same average transmit power and the same efficiency, defined as the ratio between the number of information symbols transmitted with one block, divided by the blocklength. This implies that the two methods must work with different blocklengths. Specifically, denoting by N and N_2 the blocklengths used by our method and by [21], the efficiency of our system is $\epsilon_1 = M/(N+L)$, where M is the number of information symbols contained in one block, whereas the efficiency of [21]

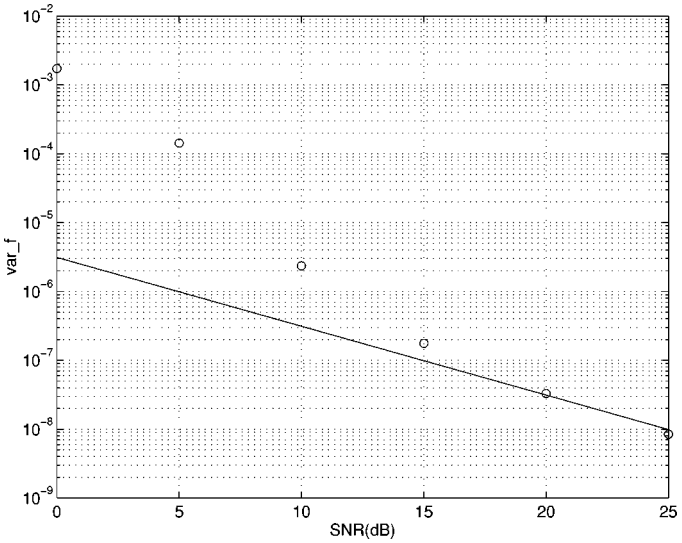

(a)

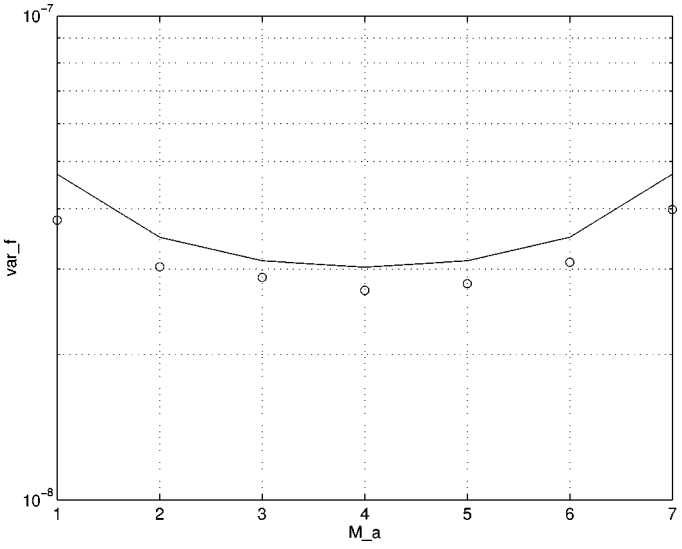

(b)

Fig. 4. Variance of frequency offset estimator in the downlink: theory (solid line) and simulation (circles); $M = 8$, $L = 2$, and $J = 8$. (a) σ_ν^2 versus SNR, $M_a = 3$. (b) σ_ν^2 versus M_a, $\mathrm{SNR} = 20$ dB.

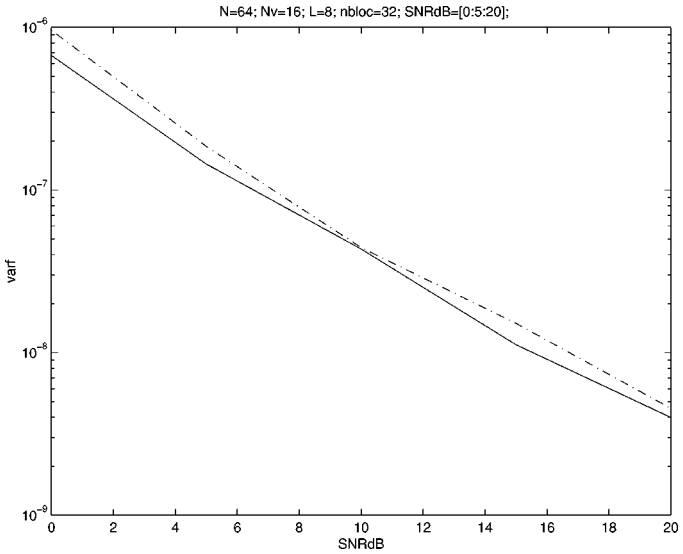

(a)

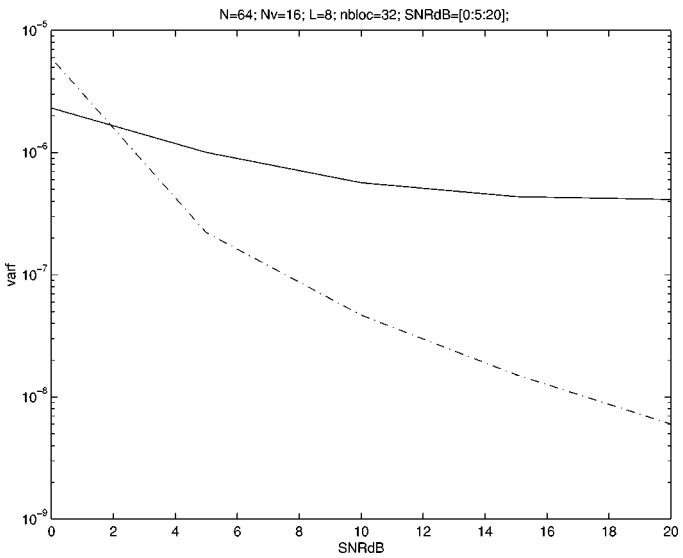

(b)

Fig. 5. Estimation variance versus SNR (dB): proposed approach (dashed line) and method of [21]. (a) Ideal channel. (b) Time-dispersive channel.

is $\epsilon_2 = N_2/(N_2 + L)$. In both cases, we use a cyclic prefix of length L. Equating the two efficiencies, we find the relationship between the blocklengths to be used in the two cases

$$N_2 = \frac{\mathrm{ML}}{N + L - M}. \tag{23}$$

In Fig. 5(a), we show the estimation error variance obtained with our approach (dashed line) and with [21] (solid line) in case of an ideal channel. The parameters are: $L = 8$, $N = 64$, $N_2 = 16$ and, thus according to (23), $M = 48$ (with $N - M = 16$ virtual subcarriers in our method). The frequency offset is the same for both systems. From Fig. 5(a) we observe that, under ideal channel conditions, the two systems perform equivalently. However, the comparison changes completely when the channel is not ideal, as testified by Fig. 5(b), where we show the variance obtained with a nonideal channel (simulated as an FIR filter whose $L + 1$ taps are complex independent Gaussian random variables) using our approach (dashed line) and the method of [21] (solid line). Furthermore, given the same efficiency and average transmitted power, we have verified that the advantages of our method increase as the blocklength increases. An intuitive explanation of this advantage is that our estimation method integrates coherently over N samples (i.e. the blocklength), whereas the method of [21] integrates over L samples, i.e. the cyclic prefix length. Therefore, for a given channel order L, as N increases with respect to L, we get better performance.

Example 3 (Frequency Estimate in the Uplink–Stationary Channel): We show now an example of performance of an uplink quasi-synchronous system, where each MU receives data from the BS with a certain $\mathrm{SNR}_{\mathrm{MU}}$ and it runs its own synchronization loop. The sequence transmitted from each MU is then affected by the residual frequency error due to imperfect synchronization. No synchronization is performed at

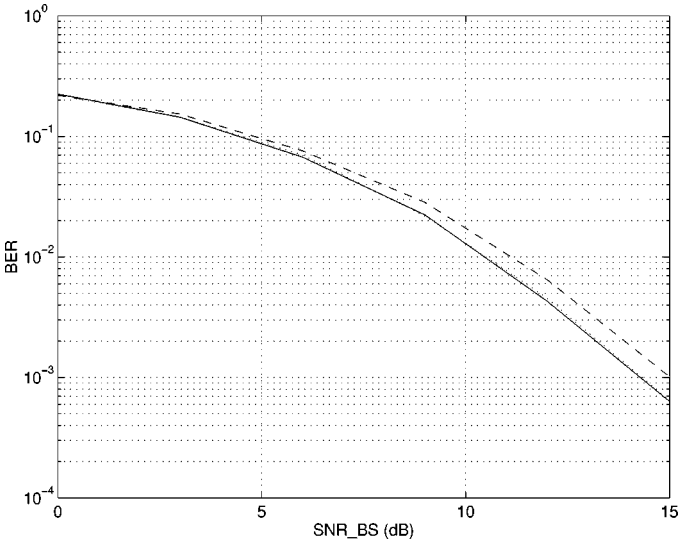

Fig. 6. BER versus $\mathrm{SNR}_{\mathrm{BS}}$ at the BS, for different values of the $\mathrm{SNR}_{\mathrm{MU}}$ at the MUs: no noise (solid line), $\mathrm{SNR}_{\mathrm{MU}} = 10$ dB (dotted line) and $\mathrm{SNR}_{\mathrm{MU}} = 5$ dB (dashed line).

the BS. The channels from each MU to the BS are independent Rayleigh channels of order $L = 2$ (we suppose that the channels have been estimated exactly, to assess the effect of the frequency synchronization errors independently of the channel estimation errors). We report in Fig. 6 the BER as a function of the $\mathrm{SNR}_{\mathrm{BS}}$ at the BS, for different values of the $\mathrm{SNR}_{\mathrm{MU}}$ at each MU (we assume for simplicity the same SNR at each MU), obtained transmitting a QPSK constellation. From Fig. 6 we observe that an $\mathrm{SNR}_{\mathrm{MU}}$ above approximately 10 dB in each MU is sufficient to guarantee a frequency synchronization error which yields a BER at the BS very close to the ideal value achievable under perfect synchronization. Interestingly, Fig. 6 shows that if the MUs have sufficient SNR (and there is no Doppler effect), there is no need for running the parallel synchronization loops at the BS.

Example 4 (Frequency Estimate in the Uplink–Nonstationary Channel): We consider now the frequency synchronization of a quasi-synchronous uplink channel, in the presence of Doppler effects, so that it is necessary to run a synchronization algorithm also at the BS. Specifically, we considered a system with parameters $M = 8$,$M_a = 4$, $L = 2$, $J = 4$,and $J_a = 16$. The frequency errors of the four users are generated as independent random variables, distributed uniformly in $(-1/2N, 1/2N)$. As an example, in Fig. 7(a) we show the errors in the estimates of the four frequency offsets pertaining to four users as a function of the iteration index, for a given channel realization and with $\mathrm{SNR} =$ 20 dB. These curves show that, thanks to the guard intervals in frequency, the parallel method estimating the frequency offset of each user separately, works fairly well. The final errors are different because the initial frequency offsets induce different interference levels to the different users. To quantify the estimation error, we report in Fig. 7(b) the variance of the frequency estimation errors of the different users versus SNR, obtained via simulation (circles). In the same curve, we show the theoretical variance (18) obtained using the same approach as in the downlink channel and assuming, ideally, that there is no interference

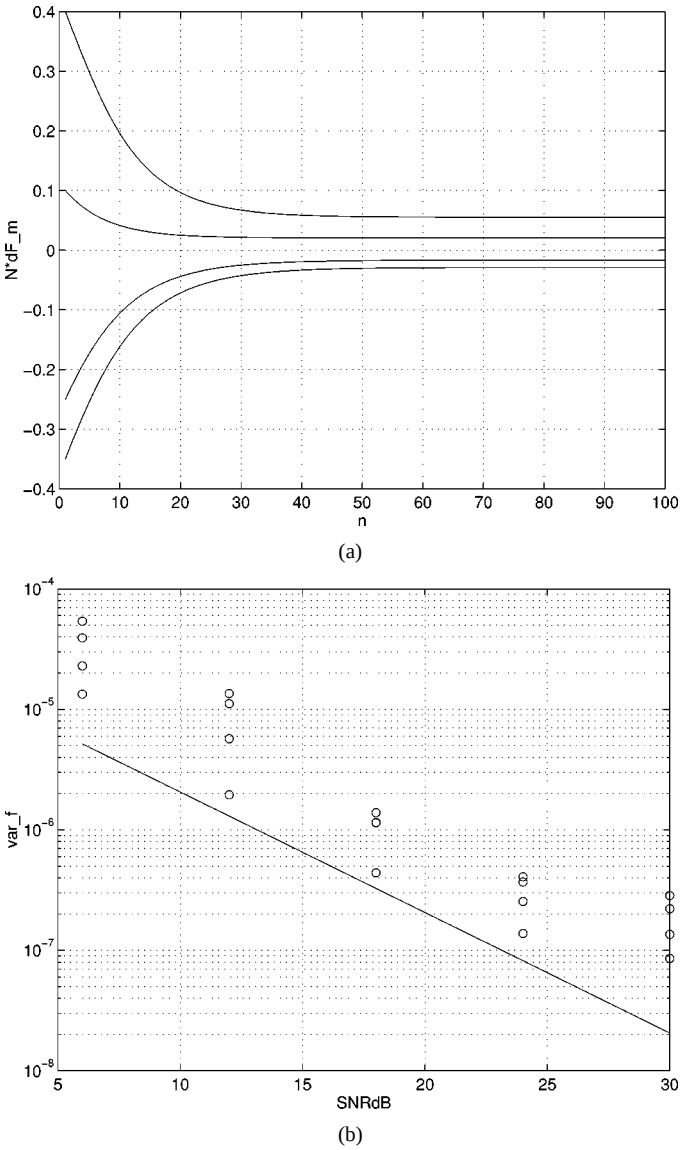

Fig. 7. Frequency estimate in the uplink channel ($M_a = 4$, $M = 8$, $L = 2$, and $J = 4$ and $J_a = 16$). (a) Residual offset versus iteration index. (b) Estimation variance for each user: simulation ("o") and theory (solid line).

among different users. From Fig. 7(b) we observe that the proposed method is able to provide small variance per user and that the theoretical expression provides a fairly good, even though optimistic, approximation of the true variance. The higher simulation values with respect to the theoretical values simply reflect the effect of the interference among users due to imperfect filtering. This is especially evident at high SNR. To improve upon this result, the BS has to send synchronization information back to the users which can then tune their oscillators, so that their residual offsets will be lower, thus allowing for a better filtering operation at the BS.

In conclusion, the synchronization scheme presented in this paper shows great potentials for multiuser OFDM. Interesting further developments include a deeper analysis of the multiple access channel, in the presence of Doppler shifts, synchronization methods for asynchronous multiple access channel, and the generalization to systems not necessarily based on OFDM, such as for example spread-spectrum CDMA systems.

APPENDIX

A. Frequency Estimation Variance

We derive an approximate closed form expression for the variance of the frequency offset estimate in the downlink channel of quasi-synchronous systems. The cost function in the presence of noise is (we drop the user index whenever it is not strictly necessary) as shown in (24) at the bottom of the page, where $\bar{y}(q;i)$ is the ideal sequence that we would receive under perfect synchronization and no noise, and it is, thus, given by (4) with $\bar{\nu}_k = 0$ and $v(q;i) = 0$; i.e.,

$$\bar{y}(q;i) = \sum_{m=0}^{M_a-1} \sum_{l=0}^{J-1} \tilde{u}_{m,k}(q;l) e^{j\frac{2\pi}{N}(m+lM+i_q)i} \tag{25}$$

where $\tilde{u}_{m,k}(q;l) := u_m(q;l)C_k(m+lM+i_q)$. From (17), the estimation variance is

$$\sigma_\nu^2 = \frac{E\left\{\left|\frac{d\delta J_{s+w}(0)}{d\nu}\right|^2\right\}}{\left|\frac{d^2 J_s(0)}{d\nu^2}\right|^2} \tag{26}$$

and, thus, we have to compute numerator and denominator of (26). We consider now an approximation of (24) valid at high SNR values, when the frequency synchronization error is small. Specifically, expanding (24) up to the second-order term in ν and retaining only the first-order noise contribution, we have

$$\begin{aligned} J_{s+w}(\nu) \approx \frac{1}{N^2 N_b} \sum_{q=1}^{N_b-1} \sum_{m'=M_a}^{M-1} \sum_{l'=0}^{J-1} \sum_{i=0}^{N-1} \sum_{i'=0}^{N-1} & [\bar{y}(q;i)\bar{y}^*(q;i') \\ & + \bar{y}(q;i)v^*(q;i') + v(q;i)\bar{y}^*(q;i')] \\ & \cdot [1 - j2\pi\nu(i-i') \\ & - 2\pi^2\nu^2(i-i')^2] e^{-j\frac{2\pi}{N}(m'+l'M+i_q)(i-i')}. \end{aligned} \tag{27}$$

Therefore, the perturbation of $J_{s+w}(\nu)$ with respect to the ideal cost function $J_s(\nu)$ observed in the absence of noise and frequency offset is as shown in (28) at the bottom of the page.

Taking the derivative of (28) with respect to ν and evaluating it at $\nu = 0$, we find that the first contribution in (28) is zero because it coincides with the derivative of the ideal cost function at $\nu = 0$, which is zero. As far as the second term is concerned, it has a zero mean value (of course up to the first-order approximation) and variance as shown in (29) at the bottom of the page. Because of the Gaussianity of the additive noise, the last two arguments of the expected value operator give zero contributions, whereas the expected value of the first term is

$$\begin{aligned} & E\{\bar{y}(q;i)\bar{y}^*(q';k)v^*(q;i')v(q';k')\} \\ & \quad = \sigma_u^2\sigma_n^2\delta[q-q']\delta[i'-k'] \\ & \qquad \times \sum_{m=0}^{M_a-1}\sum_{l=0}^{J-1} |C(m+lM+i_q)|^2 e^{j2\pi(m+lM+i_q)(i-k)/N} \end{aligned} \tag{30}$$

where $\delta[i]$ is the unit pulse. Moreover, $E\{v^*(q;i')v(q';k')\} = \sigma_n^2\delta[q-q']\delta[i'-k']$, and

$$\begin{aligned} & E\{\bar{y}(q;i)\bar{y}^*(q';k)\} \\ & \quad = \sum_{m=0}^{M_a-1}\sum_{l=0}^{J-1}\sum_{m'=0}^{M_a-1}\sum_{l'=0}^{J-1} E\{\tilde{u}_{m,k}(q;l)\tilde{u}^*_{m',k'}(q';l')\} \\ & \qquad \times e^{j\frac{2\pi}{N}[(m+lM+i_q)i-(m'+l'M+i_{q'})k]} \end{aligned} \tag{31}$$

where

$$\begin{aligned} & E\{\tilde{u}_{m,k}(q;l)\tilde{u}^*_{m',k'}(q';l')\} \\ & \quad = \sigma_u^2 |C(m+lM+i_q)|^2 \delta[m-m']\delta[l-l']\delta[q-q']. \end{aligned} \tag{32}$$

To evaluate the summation over q of the expected value in (29), we recall that we have chosen N_b as an integer multiple of N, let us say $N_b = KN$. We then have $(1/N_b)\sum_{q=0}^{N_b-1} |C(m+lM+i_q)|^2 e^{j2\pi i_q(i-k)/N} e^{-j2\pi i_q(i-i'-k+k')/N} = C^2$, since the sum $C^2 := \sum_{q=1}^{N} |C(m+lM+i_q)|^2$ does not depend on m, or on l, provided that i_q, for $q = 0, \ldots, N-1$, spans all the values

---

$$J_{s+w}(\nu) = \frac{1}{N_b}\sum_{q=1}^{N_b-1}\sum_{m'=M_a}^{M-1}\sum_{l'=0}^{J-1}\left|\frac{1}{N}\sum_{i=0}^{N-1}(\bar{y}(q;i)+v(q;i))e^{j2\pi\nu(q(N+L)+i)}e^{-j\frac{2\pi}{N}(m'+l'M+i_q)i}\right|^2 \tag{24}$$

$$\begin{aligned} \delta J_{s+w}(\nu) \approx \frac{1}{N^2 N_b} \sum_{q=1}^{N_b-1} \sum_{m'=M_a}^{M-1} \sum_{l'=0}^{J-1} \sum_{i=0}^{N-1} \sum_{i'=0}^{N-1} & [\bar{y}(q;i)\bar{y}^*(q;i')(-j2\pi\nu(i-i') - 2\pi^2\nu^2(i-i')^2) + (\bar{y}(q;i)v^*(q;i') \\ & + v(q;i)\bar{y}^*(q;i'))(1 - j2\pi\nu(i-i') - 2\pi^2\nu^2(i-i')^2)] e^{-j\frac{2\pi}{N}(m'+l'M+i_q)(i-i')} \end{aligned} \tag{28}$$

$$\begin{aligned} E\left\{\left|\frac{d\delta J_{s+w}(0)}{d\nu}\right|^2\right\} = \frac{4\pi^2}{N^4 N_b^2} \sum_{q,q'=1}^{N_b-1} \sum_{m',m''=M_a}^{M-1} \sum_{l',l''=0}^{J-1} \sum_{i,i'=0}^{N-1} \sum_{k,k'=0}^{N-1} & E\{\bar{y}(q;i)\bar{y}^*(q';k)v^*(q;i')v(q';k') \\ & + \bar{y}^*(q;i')\bar{y}(q';k')v(q;i)v^*(q';k) + \bar{y}(q;i)\bar{y}(q';k')v^*(q;i')v^*(q,k) \\ & + \bar{y}^*(q;i')\bar{y}^*(q';k)v(q;i)v(q';k')\} \cdot (i-i')(k-k') e^{-j\frac{2\pi}{N}[(m'+l'M+i_q)(i-i')-(m''+l''M+i_{q'})(k-k')]} \end{aligned} \tag{29}$$

$$E\left\{\left|\frac{d\delta J_{s+w}(0)}{df}\right|^2\right\} = \frac{8\pi^2\sigma_u^2C^2\sigma_n^2}{N^4}\sum_{m'=M_a}^{M-1}\sum_{m''=M_a}^{M-1}\sum_{l'=0}^{J-1}\sum_{l''=0}^{J-1}\sum_{i=0}^{N-1}\sum_{i'=0}^{N-1}\sum_{k=0}^{N-1}(i-i')(k-k') \cdot \sum_{m=0}^{M_a-1}\sum_{l=0}^{J-1} e^{j2\pi(m+lM)(i-k)/N}e^{j2\pi(m'-m''+(l'-l'')M)i'/N}e^{-j2\pi[(m'+l'M+)i-(m''+l''M+)i]/N} \quad (33)$$

between 0 and $N-1$, because $C(m+lM+i_q)$ is periodic of period N. Therefore, considering the similarity of the first two terms in (29), we can rewrite (29) as shown in (33) at top of the page. Carrying out the summations over m', m'', l', and l'', after a few algebraic manipulations we obtain

$$E\left\{\left|\frac{d\delta J_{s+w}(0)}{df}\right|^2\right\} = \frac{8\pi^2\sigma_u^2J^6C^2\sigma_n^2}{N^4}\sum_{n=0}^{M-1}\sum_{p=0}^{M-1}\sum_{q=0}^{M-1}(n-p)(q-p) \cdot \frac{\sin[\pi M_a(n-q)/M]}{\sin[\pi(n-q)/M]}\frac{\sin[\pi M_a(n-p)/M]}{\sin[\pi(n-p)/M]} \times \frac{\sin[\pi M_a(q-p)/M]}{\sin[\pi(q-p)/M]}. \quad (34)$$

Proceeding similarly, we also get

$$\left|\frac{d^2J_s(0)}{d\epsilon_f^2}\right|^2 = \frac{16\pi^4\sigma_u^4C^4J^{10}}{N^4} \times \sum_{n=0}^{M-1}\sum_{p=0}^{M-1}(n-p)^2\frac{\sin^2[\pi M_a(n-p)/M]}{\sin^2[\pi(n-p)/M]}. \quad (35)$$

Substituting now (34) and (35) in (26), we get the variance (18).

B. Step Size

The frequency update in the nth iteration cycle is (we drop the user index for simplicity of notation)

$$\nu(n+1) = \nu(n) - \mu\frac{dJ(\nu(n))}{d\nu(n)}. \quad (36)$$

Taking the second-order series expansion of $dJ(\nu(n))/d\nu$ in the neighborhood of 0, we have $dJ(\nu(n))/d\nu(n) = \lambda\nu(n)$, with

$$\lambda = -\frac{4\pi^2\sigma_u^2C^2}{N^2}\sum_{i=0}^{N-1}\sum_{i'=0}^{N-1}(i-i')^2\,\mathrm{sinc}_{M_a}(\pi(i-i')M_a/N) \times \mathrm{sinc}_{M-M_a}(\pi(i-i')M - M_a/N)\,\mathrm{sinc}_J^2(\pi(i-i')/J). \quad (37)$$

Iterating the method, we have

$$\nu(n+1) = \nu(n)(1-\mu\lambda) = \cdots = \nu(0)(1-\mu\lambda)^{n+1}. \quad (38)$$

Therefore, the method converges if $|1-\mu\lambda| < 1$; i.e., if $0 < \mu < 2/\lambda$, with λ given by (37).

REFERENCES

[1] F. Classen and H. Meyr, "Frequency synchronization algorithms for OFDM systems suitable for communication over frequency-selective fading channel," in *Proc. 44th Vehicular Technology Conf.*, 1994, pp. 1655–1659.

[2] F. Daffara and O. Adami, "A new frequency detector for orthogonal multicarrier transmission techniques," in *Proc. IEEE Vehicular Technology Conf.*, 1995, pp. 804–809.

[3] "Broadband Radio Access Networks (BRAN)—Inventory of Broadband Radio Technologies and Techniques," Eur. Telecommun. Standardization Inst. (ETSI), Sophia Antipolis, France, Tech. Rep. DTR/BRAN-030 001, 1998.

[4] K. Fazel and G. Fettweis, Eds., *Multi-carrier Spread-Spectrum*. Norwell, MA: Kluwer Academic, 1997.

[5] G. B. Giannakis, Z. Wang, A. Scaglione, and S. Barbarossa, "AMOUR-generalized multicarrier transceiver for blind CDMA regardless of multipath," *IEEE Trans. Commun.*, vol. 48, pp. 2064–2076, Dec. 2000.

[6] L. Hanzo, W. Webb, and T. Keller, *Single and Multicarrier Quadrature Amplitude Modulation*. New York: Wiley, Apr. 2000.

[7] T. Keller, L. Piazzo, P. Mandarini, and L. Hanzo, "Orthogonal frequency division multiplex synchronization techniques," *IEEE J. Select. Areas Commun.*, vol. 19, pp. 999–1008, June 2001.

[8] U. Lambrette, M. Speth, and H. Meyr, "OFDM burst frequency synchronization by single carrier training data," *IEEE Commun. Lett.*, vol. 1, pp. 46–48, Mar. 1997.

[9] D. Lee and K. Cheun, "A new symbol timing recovery algorithm for OFDM systems," *IEEE Trans. Consumer Electron.*, vol. 43, pp. 767–775, Aug. 1997.

[10] H. Liu and U. Tureli, "A high-efficiency carrier estimator for OFDM communication," *IEEE Commun. Lett.*, vol. 2, pp. 104–106, Apr. 1998.

[11] M. Luise and R. Reggianini, "Carrier frequency acquisition and tracking for OFDM systems," *IEEE Trans. Commun.*, vol. 44, pp. 1590–1598, Nov. 1996.

[12] P. Moose, "A technique for orthogonal frequency division multiplexing frequency offset correction," *IEEE Trans. Commun.*, vol. 42, pp. 2908–2914, Oct. 1994.

[13] M. Morelli and U. Mengali, "An improved frequency offset estimator for OFDM applications," *IEEE Commun. Lett.*, vol. 3, pp. 75–77, Mar. 1999.

[14] J. S. Oh, Y. M. Chung, and S. U. Lee, "A carrier synchronization technique for OFDM on the frequency-selective fading environment," in *Conf. Rec. VTC*, 1996, pp. 1574–1578.

[15] T. Pollet, M. V. Bladel, and M. Moeneclaey, "BER sensitivity of OFDM systems to carrier frequency offset and wiener phase noise," *IEEE Trans. Commun.*, vol. 43, pp. 191–193, Feb., Mar., Apr. 1995.

[16] H. Roh, K. Cheun, and J. Park, "An MMSE fine carrier frequency synchronization algorithm for OFDM systems," *IEEE Trans. Consumer Electron.*, vol. 43, pp. 761–766, Aug. 1997.

[17] G. Santella, "A frequency and symbol synchronization system for OFDM signals: Architecture and simulation results," *IEEE Trans. Commun.*, vol. 49, pp. 254–275, Jan. 2000.

[18] H. Sari and G. Karam, "Orthogonal frequency-division multiple access and its application to CATV networks," *Eur. Trans. Telecommun.*, vol. 9, no. 6, pp. 507–516, Nov.–Dec. 1998.

[19] T. M. Schmidl and D. C. Cox, "Robust frequency and timing synchronization for OFDM," *IEEE Trans. Commun.*, vol. 45, pp. 1613–1621, Dec. 1997.

[20] U. Tureli, H. Liu, and M. Zoltowski, "OFDM blind carrier offset estimation: ESPRIT," *IEEE Trans. Commun.*, vol. 48, pp. 1459–1461, Sept. 2000.

[21] J. J. Van de Beek, M. Sandell, and P. O. Borjesson, "ML estimation of time and frequency offset in OFDM systems," *IEEE Trans. Signal Processing*, vol. 45, pp. 1800–1805, July 1997.

[22] J. J. Van de Beek, P. O. Borjesson, M. L. Boucheret, D. Landström, J. M. Arenas, P. Ödling, C. Östberg, M. Wahlqvist, and S. K. Wilson, "A time and frequency synchronization scheme for multiuser OFDM," *IEEE J. Select. Areas Commun.*, vol. 17, pp. 1900–1913, Nov. 1999.
[23] S. Verdú, "Wireless bandwidth in the making," *IEEE Commun. Mag.*, vol. 38, pp. 53–58, July 2000.
[24] ——, *Multiuser Detection*. Cambridge, U.K.: Cambridge Univ. Press, 1998.
[25] Z. Wang and G. B. Giannakis, "Wireless multicarrier communications: Where fourier meets shannon," *IEEE Signal Processing Mag.*, vol. 17, pp. 29–48, May 2000.
[26] W. D. Warner and C. Leung, "OFDM/FM frame synchronization for mobile radio data communication," *IEEE Trans. Veh. Technol.*, vol. 42, pp. 302–313, Aug. 1993.
[27] L. Wei and C. Schelegel, "Synchronization requirements for multiuser OFDM on satellite mobile and two-path Rayleigh fading channels," *IEEE Trans. Commun.*, vol. 43, pp. 887–895, Feb./Mar./Apr. 1995.

Sergio Barbarossa (S'82–M'88) graduated in electrical engineering and received the Ph.D. degree from the University of Rome "La Sapienza," Rome, Italy, in 1984 and 1989, respectively.

In 1985, he joined the Radar System Division of Selenia, Rome, Italy, where he was a Radar System Engineer. From November 1987 to August 1988, he was a Research Engineer at the Environmental Research Institute of Michigan (ERIM), Ann Arbor, where he was involved in research activities on synthetic aperture radars. From 1988 to October 1991, he was an Adjunct Professor at the University of Perugia, Italy and in November 1991, he joined the University of Rome "La Sapienza" where he is now a Full Professor. He is currently responsible for the university's team working on two international projects on wireless broadband networks using CDMA, space-time coding, and multihop networks. His current research interests lie in the area of signal processing for digital communications, multiple access methods, space-time coding, multihop networks, and communications over time-varying channels.

Dr. Barbarossa has served as an Associate Editor for the IEEE TRANSACTIONS ON SIGNAL PROCESSING and, since 1997, he is a member of the *IEEE Signal Processing for Communications Technical Committee*. He is co-recipient of the 2000 IEEE Best Paper Award from the IEEE Signal Processing Society for a paper in Signal Processing for Communications.

Massimiliano Pompili was born in 1973. He receieved the electrical engineering degree from the University of Rome "La Sapienza," Rome, Italy, in 2000.

After graduation, he collaborated with the INFOCOM Department of the University of Rome "La Sapienza" on a joint research on the synchronization of multiple access systems. Since October 2001, he is with Marconi Mobile, Rome, Italy. His research interests lie in the field of wireless communications, code division multiple access, and synchronization.

Georgios B. Giannakis (S'84–M'86–SM'91–F'97) received the Diploma in Electrical Engineering from the National Technical University of Athens, Athens, Greece, in 1981.

From September 1982 to July 1986 he was with the University of Southern California (USC), Los Angeles, where he received the M.Sc. degree in electrical engineering, 1983. He received the M.Sc. degree in mathematics and the Ph.D. degree in electrical engineering, from USC in 1983 and 1986, respectively.

After lecturing for one year at USC, he joined the University of Virginia, Charlottesville, in 1987, where he became a Professor of Electrical Engineering in 1997. Since 1999, he has been with the University of Minnesota, Minneapolis, as a Professor of Electrical and Computer Engineering. His general interests span the areas of communications and signal processing, estimation and detection theory, time-series analysis, and system identification. He has published more than 120 journal papers, 250 conference papers, and two edited books on these subjects. His current research topics focus on transmitter and receiver diversity techniques for single-user and multiuser fading communication channels, redundant precoding and space-time coding for block transmissions, multicarrier, and wide-band wireless communication systems. He is a frequent consultant for the telecommunications industry.

Dr. Giannakis is the (co-) recipient of three best paper awards from the IEEE Signal Processing (SP) Society (1992, 1998, and 2000). He also received the Society's Technical Achievement Award in 2000. He co-organized three IEEE-SP Workshops (HOS in 1993, SSAP in 1996 and SPAWC in 1997) and guest (co-) edited four special issues. He has served as an Associate Editor for the IEEE TRANSACTIONS ON SIGNAL PROCESSING and the IEEE SIGNAL PROCESSING LETTERS, a secretary of the SP Conference Board, a member of the SP Publications Board and a member and vice-chair of the Statistical Signal and Array Processing Committee. He is a member of the Editorial Board for the PROCEEDINGS OF THE IEEE, he chairs the SP for Communications Technical Committee and serves as the Editor in Chief for the IEEE SIGNAL PROCESSING LETTERS. He is a member of the IEEE Fellows Election Committee, the IEEE-SP Society's Board of Governors.